SSRG International Journal of Electrical and Electronics Engineering
ISSN: 2348-8379/ https://doi.org/10.14445/23488379/IJEEE-V11I11P115

Volume 11 Issue 11, 139-149, November 2024

Original Article

Performance Enhancement of PMSG Wind Farm with Adaptive Fuzzy-Based PID Regulator in Non-Linear Backstepping Controller

Banothu.Balasubramanyam[1], Balasubbareddy Mallala[2], G. Mallesham[3]

[1]*Department of Electrical Engineering, Osmania University, Hyderabad, Telangana, India.*
[2]*Department of Electrical & Electronics Engineering, Chaitanya Bharathi Institute of Technology, Hyderabad, Telangana, India.*
[3]*Department of Electrical Engineering, Osmania University, Hyderabad, Telangana, India.*

[1]*Corresponding Author : balumahendrabanothu@gmail.com*

Received: 09 September 2024 Revised: 10 October 2024 Accepted: 08 November 2024 Published: 30 November 2024

Abstract *- PMSG wind farms are considered the most reliable renewable energy sources as they can generate high-rating power for a small area installation. Due to the machine's structure with a permanent magnet rotor, it becomes a standalone source with no dependency on the grid. Due to this, the transients and damping during initial operating conditions are also high, generating peak voltages and currents at the initial stage. This paper integrates an adaptive fuzzy-based PID regulator into the non-linear backstepping control of the grid side converter for voltage stability. The controller is initially modelled with conventional PI and fuzzy regulators, and the performance is observed. A comparative analysis between different regulators is carried out and updated in the grid-side converter control. There will be a significant improvement in the DC voltage regulation at the DC link of the back-to-back connected converters. With the adaptive fuzzy PID regulator, the peak overshoot of the DC voltage will be gradually dropped, the desired voltage will have a faster settling time, and the ripple content will be reduced. As per these improvements, the performance of the PMSG wind farm with back-to-back connected converters has been enhanced. All the comparative analysis and modeling of the regulators are done using MATLAB Simulink software using 'Powersystems' blocks of the Simulink library. The analysis shows that the AF-PID controller has a faster response to the changes in the system. The initial and transient recovery peak overshoots, ripple and harmonics in the voltages are reduced to a greater extent with the proposed controller.*

Keywords *- Permanent Magnet Synchronous Generator (PMSG), Adaptive fuzzy Proportional Integral Derivative (PID), MATLAB simulink.*

1. Introduction

In the near future, most power generation will be done through renewable sources, replacing conventional fossil fuel power generation [1]. Renewable power generation has zero carbon emissions and uses only natural sources for electrical power production. The most promising and high-rated renewable source of many available renewable sources is wind farms [2].

Wind farms need a lesser installation area for a given power rating than solar plants or biogas plants. Many types of wind farms have different machines coupled to the wind turbine. The asynchronous machines are considered the most efficient and stable generators and are very optimal for wind farm applications. However, the asynchronous machines (wound or squirrel) need initial active and reactive powers for excitation.

Moreover, the machine always needs to be connected to the grid for synchronous operation and for creating a rotating magnetic field. These issues can be overcome by the PMSM connected to the wind turbine, which generates power individually without any external excitation [3].

The PMSMs are considered the most efficient and independent generators with immediate power generation during initial states. The permanent magnet rotor of the machine makes it more optimal for application in wind farms. The major drawback of PMSM is its instability and high sensitivity to the changes in the wind turbine speed. The wind speed depends on the propeller speed, which varies per wind speed [4].

The sudden change in the turbine speeds will lead to variations in the PMSM voltages and frequency. Many

disturbances and oscillations are created if the PMSM is directly connected to the grid as an asynchronous machine. This leads to harmonic generation, damaging the modules connected to the grid [5].

The PMSM voltage needs to be stabilized using power electronic circuits controlled by synchronization controllers. Recent advancements in control strategies for PMSG wind farms aim to improve efficiency, enhance grid stability, and reduce power fluctuations. Techniques such as Model Predictive Control (MPC) and nonlinear MPPT algorithms have increased the accuracy of tracking the maximum power point, even under rapidly changing wind conditions. Advanced algorithms also enable PMSG systems to participate actively in frequency and voltage regulation. This includes the use of droop control techniques and synthetic inertia mechanisms.

Additionally, advanced filtering methods integrated with the converter help reduce harmonics, lowering overall distortion in power output. Algorithms like repetitive control and multi-resonant control further mitigate harmonics introduced by switching operations in converters, improving the quality of power delivered to the grid. In wind farms with multiple PMSG units, decentralized control minimizes the need for centralized communication, making the system more robust and scalable.

A back-to-back connected six switch Voltage Source Converters (VSCs) are used for the voltage stabilization and synchronization of the PMSM-based wind turbine. A DC capacitor is included at the DC link of the back-to-back connected VSC for voltage ripple reduction and disturbance control. Both the VSCs are named as Machine Side Converter (MSC) and Grid Side Converter (GSC) [6]. The MSC operates in synchronization with the PMSM rotor angle tetham (θ_r) and the GSC operates in synchronization with the grid voltage phase angle (θ_g). The circuit topology of the PMSM-based wind turbine with six switch back-to-back connected VSCs is presented in Figure 1.

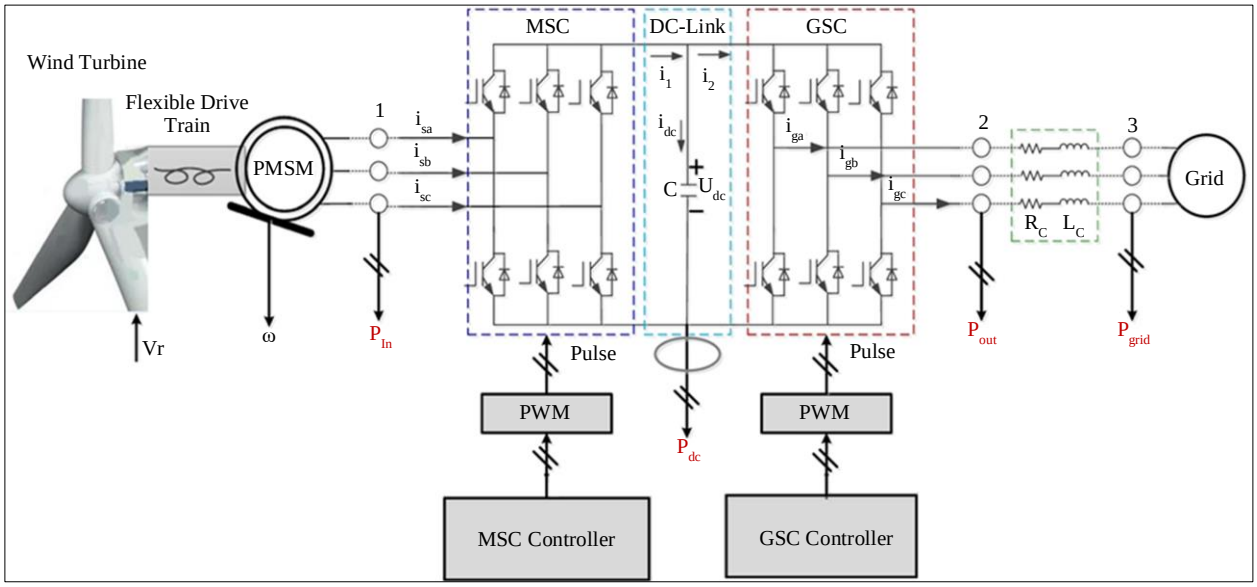

Fig. 1 PMSM-based wind turbine generator circuit topology

As represented in Figure 1, the PMSM is connected to a six-switch VSC (MSC), which rectifies the three phase voltages of the PMSM. The converted DC voltage is inverted to three phase AC voltages by the GSC based on the grid's voltage magnitude, phase, and frequency. The DC link voltage is stabilized by the non-linear backstepping GSC controller [7].

The rectification operation is controlled by the non-linear backstepping MSC controller, which operates in synchronization with the PMSM rotor angular speed. At the DC link, a high-value capacitance is provided to ensure stable DC link voltage at the specified value in the GSC controller [8]. The conventional PI controller is updated with an adaptive fuzzy PID regulator for optimal DC voltage regulation. Previous research also considered a comparative analysis using PI and a fuzzy logic controller.

The paper is organized with an introduction to the PMSM-based wind turbine structure and details of modules included in the proposed system in Section 1. Section 2 has the control design and configuration of MSC and GSC non-linear backstepping controllers, followed by Section 3. Section 3 includes the adaptive fuzzy PID-based DC voltage regulator design. A comparative simulation analysis with different DC voltage regulators in the GSC controller is presented in section 4. The results are generated using MATLAB Simulink software with blocks considered from the

Simulink browser. The optimal DC voltage regulator is determined by the simulation results of the models. The results are validated in the final Section 5, which is the conclusion to the paper, followed by references cited.

2. Non-Linear Backstepping Control

As mentioned previously in section 1, the PMSM-based wind turbine generator cannot be connected directly to the grid due to the instability of the machine. With changing speeds of the turbine, the output characteristics of PMSM vary drastically, which can create many power quality issues in the grid to which it is connected [9]. Even with variable power generation, the voltage output of the machine needs to be ensured to be stable. The generated power (P_g) by the wind generator is given as:

$$P_g = \frac{1}{2}\left(C_1\left(\frac{C_2}{\lambda}\, C_3\beta - C_4\right)e^{\frac{-C_5}{\lambda'}} + C_6\lambda'\right)\rho S V_w^3 \quad (1)$$

$$\frac{1}{\lambda'} = \frac{1}{\lambda+0.08\beta} - \frac{0.035}{\beta^3+1} \quad (2)$$

Here, $C_{1\text{-}6}$ are the power coefficients, λ is the tip speed ratio, β blade pitch angle, S is the sensitivity factor, and V_w is the wind speed. The PMSM can never be synchronized to the grid when connected directly for any speed input and mechanical power input to the machine. Therefore, a two-stage conversion system with power electronic circuits is integrated into the PMSM for power extraction, conversion and injection to the grid in synchronization [10].

As presented in Figure 1, back-to-back VSCs are used to achieve the task. These back-to-back converters (MSC and GSC) are controlled by the Sinusoidal PWM (Pulse Width Modulation) technique. The PWM needs to reference three-phase Sinusoidal signals to generate pulses for the MSC or GSC IGBT switches. These reference signals are generated by individual non-linear backstepping controllers controlling the back-to-back VSCs for synchronized power extraction and sharing to the grid [11]. The control structure of the proposed non-linear backstepping controller with feedback signals from the machine and the grid is presented in Figure 2.

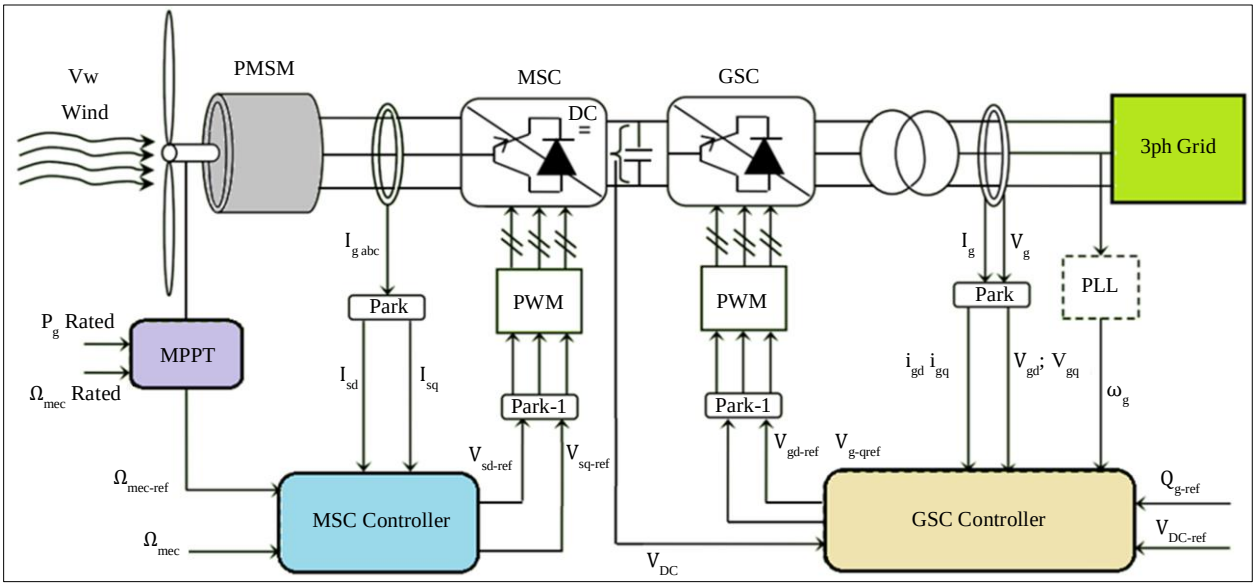

Fig. 2 MSC and GSC control structures

The PWM generators of the MSC and GSC controller need individual 'abc' reference Sinusoidal signals [11]. These 'abc' signals are generated by the Inverse Park's transformation of the dq voltage signals given as:

$$V_{sd-ref} = \frac{1}{2}\gamma_\Omega^2 \quad (3)$$

$$V_{sq-ref} = \frac{1}{2}(\gamma_\Omega^2 + \gamma_d^2 + \gamma_q^2) \quad (4)$$

$$V_{gd-ref} = R_g.i_{gd} - L_g\omega_g.i_{gq} - L_gK_{gd}.\gamma_{gd} + V_{gd} \quad (5)$$

$$V_{gq-ref} = R_g.i_{gq} + L_g\omega_g.i_{gd} - L_gK_{gq}.\gamma_{gq} + V_{gq} \quad (6)$$

Here, V_{sd-ref} and V_{sq-ref} are the reference dq signals for the MSC, V_{gd-ref} and V_{gq-ref} are the reference dq signals for GSC [12]. In Equation (3) γ_Ω is given as:

$$\gamma_\Omega = \Omega_{mec\,ref} - \Omega_{mec} \quad (7)$$

Here, $\Omega_{mec\,ref}$ is the reference rotor speed and Ω_{mec} is the measured rotor speed of PMSM. The $\Omega_{mec\,ref}$ is estimated as:

$$\Omega_{mec\,ref} = \frac{V_w.\lambda}{R} \quad (8)$$

Here R is the turbine blade radius. The $\gamma_d \gamma_q$ are calculated as:

$$\gamma_d = i_{sd-ref} - i_{sd}\ ; \gamma_q = i_{sq-ref} - i_{sq} \quad (9)$$

Here, i_{sd} and i_{sq} are the measured dq components of the PMSM stator currents (I_{Sabc}) [13]. i_{sd-ref} and i_{sq-ref} are the reference dq current components given as:

$$i_{sd-ref} = 0\ ; i_{sq-ref} = -\frac{T_{em}}{\varphi} \quad (10)$$

The i_{sd-ref} is taken as zero, representing no active power consumption during power generation. The T_{em} is the electromagnetic torque, and φ is the flux linkages of the PMSM. In Equations (5) and (6) R_g and L_g are the grid impedance (resistance and inductance). ω_g is the grid angular frequency given as $2\pi f_g$, where f_g is the grid frequency. i_{gd} i_{gq} and $V_{gd} V_{gq}$ are the grid currents and voltages dq components achieved by Park's transformations. γ_{gd} γ_{gq} are given as:

$$\gamma_{gd} = i_{gd-ref} - i_{gd}\ ; \gamma_{gq} = i_{gq-ref} - i_{gq} \quad (11)$$

The i_{gd-ref} i_{gq-ref} reference current components as calculated as:

$$i_{gd-ref} = (V_{dc-ref} - V_{dc})\left(K_{pv} + \frac{K_{iv}}{s}\right);$$

$$i_{gq-ref} = -\frac{Q_{g-ref}}{1.5\,V_{gq}} \quad (12)$$

With no reactive power exchange between the grid and PMSM, the $Q_{g-ref} = 0$, which makes $i_{gq-ref} = 0$. The i_{gd-ref} is calculated from the voltage regulator of the DC link voltage. V_{dc-ref} and V_{dc} are the reference and measured DC link voltages. K_{pv} and K_{iv} are the proportional and integral gains of conventional PI DC voltage regulators [14].

From the given equations of the non-linear backstepping controller design, the proposed wind turbine is analysed with different DC voltage regulators (Fuzzy and Adaptive fuzzy PID). The voltage regulators are tuned accordingly for system performance enhancement with lower disturbances and harmonics.

3. Adaptive Fuzzy PID Regulator

The adaptive fuzzy PID regulator is the hybrid controller with PID controlled by a Fuzzy logic controller. The controller has all the advantages of the PID controller along with faster response using the Fuzzy logic control. The input to this Hybrid adaptive Fuzzy PID regulator is the error DC voltage in the GSC controller [15]. As per the gains given by the PID controller (Kp Ki Kd), Membership Functions (MFs), and rule base of the Fuzzy controller, the output is controlled. The structure of the proposed adaptive fuzzy PID regulator in the GSC controller is presented in Figure 3.

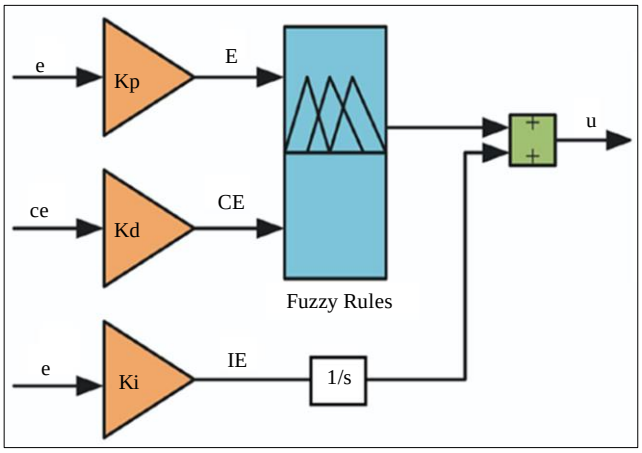

Fig. 3 Adaptive fuzzy PID controller structure

In Figure 3, the inputs to the Fuzzy logic controller are 'error' (e) and 'change in error' (ce) fed through Kp and Kd gains, respectively. The 'e' and 'ce' signals are calculated as:

$$e = V_{dc-ref} - V_{dc}\ ; ce = e(k) - e(k-1) \quad (13)$$

Here, e(k) and e(k-1) are the present and previous error values. The previous value is generated by a 'delay' block set at the output of the 'e' signal [16]. The same 'e' signal is also fed to integral gain Ki with an integrator (1/s), which is added to the output of the Fuzzy controller.

Each input variable of the Fuzzy logic controller is set with specified MFs and ranges for controlling the output value. Each input and output variable has seven MFs transformed to triangular shape MFs using the 'mamdani' type Fuzzy. The ranges of these variables are taken as per the input range and expected output value. The MFs design of the input and output variables is presented in Figure 4.

As presented, each MFs of the variable is set with a specified range, creating equal regions. The MFs are named as 'Negative Big (NB)', 'Negative Medium (NM)', 'Negative Small (NS)', 'Zero (Z)', 'Positive Small (PS)', 'Positive Medium (PM)', 'Positive Big (PB)' [17]. The ranges of the MFs of each variable are given in Table 1. These MFs with specified ranges are set with a 49 If-Then rule base for generating the output value as per the given AND logic [18]. The 49 rule base for the given MFs is presented in Table 2.

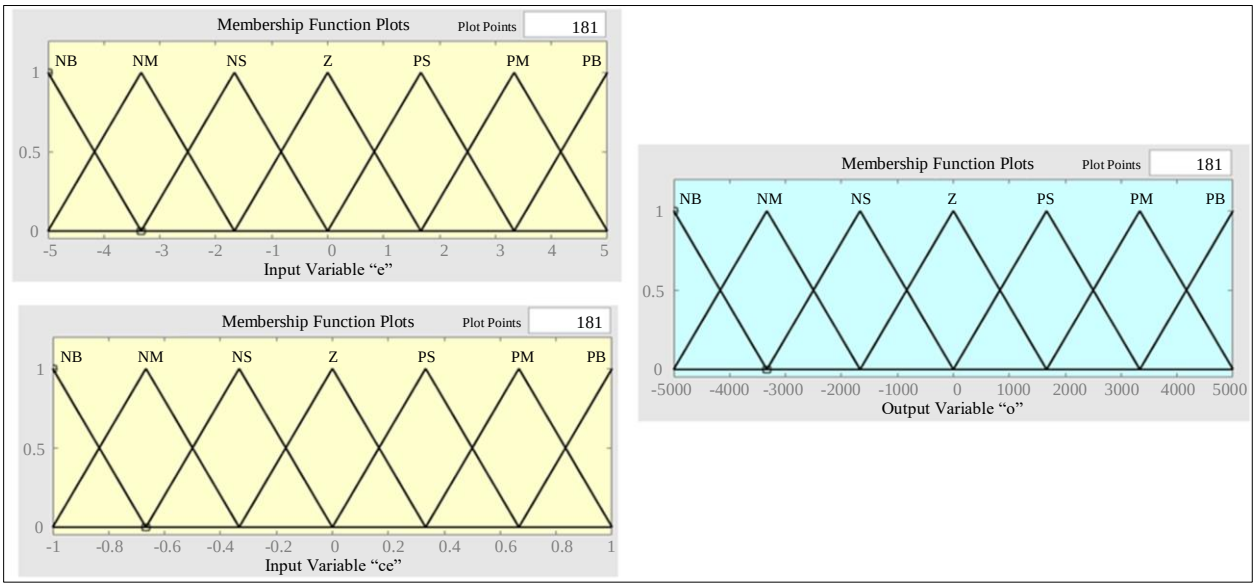

Fig. 4 Input and output variable MFs of fuzzy logic controller

Table 1. MFs ranges

MFs Name	Range of 'e'	Range of 'ce'	Range of 'o'
NB	[-6.665 -5 -3.333]	[-1.333 -1 -0.6666]	[-6665 -5000 -3333]
NM	[-5 -3.333 -1.667]	[-1 -0.667 -0.333]	[-5000 -3333 -1667]
NS	[-3.333 -1.667 0]	[-0.6666 -0.3334 0]	[-3333 -1667 0]
Z	[-1.667 0 1.667]	[-0.3334 0 0.3334]	[-1667 0 1667]
PS	[0 1.667 3.333]	[0 0.3334 0.6666]	[0 1667 3333]
PM	[1.667 3.333 5]	[0.3334 0.6666 1]	[1667 3333 5000]
PB	[3.333 5 6.67]	[0.6666 1 1.334]	[3333 5000 6670]

Table 2. Rule base

'49 Rule Base'		Error 'e'						
		NB	NM	NS	Z	PS	PM	PB
Change in Error 'ce'	PB	Z	PS	PM	PB	PB	PB	PB
	PM	NS	Z	PS	PM	PB	PB	PB
	PS	NM	NS	Z	PS	PM	PB	PB
	Z	NB	NM	NS	Z	PS	PM	PB
	NS	NB	NB	NM	NS	Z	PS	PM
	NM	NB	NB	NB	NM	NS	Z	PS
	NB	NB	NB	NB	NB	NM	NS	Z

As per the given rule table, the output 'o' is generated. The output range is tuned as per the response of the voltage regulator to the input given to the controller [19]. The surface of the 49-rule base is presented in Figure 5. The PI or fuzzy-based voltage regulator in the GSC controller is replaced by the designed adaptive fuzzy PID regulator for better performance of the PMSM-based wind turbine generator. A comparative analysis between different controllers is presented in the following section with time-dependent graphs.

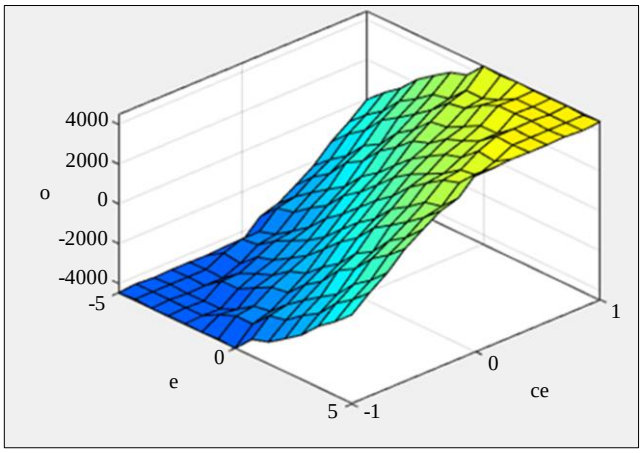

Fig. 5 Surface of the 49-rule base

4. Result and Analysis

The proposed system with a PMSM base wind turbine generator operated with back-to-back VSCs for voltage stability is designed and modeled using blocks from the Simulink library of MATLAB software. All the blocks are considered from the 'Simpowersystems' subset, which include 'machines', 'power electronics', 'passives', 'electrical sources' and 'measurements'. The considered Simulink block values are updated with the given configuration parameters in Table 3.

Table 3. Configuration parameters

Name of the module	Parameter values
Grid	11kV 50Hz 100MVA Step down T/F = 11kV/1.5kV, 50Hz, 2.5MVA
PMSG	P_n = 2MW, V_n = 1.5kV, R_s = 0.0304, $L_d = L_q$ = 1.8mH, flux = 4.633, J = 300000, N_p = 75, w_{rated} = 4.1888, Rf = 0.0034Ω, Lf = 0.0011H, Cf = 120kVAR.
Wind Turbine	Pn = 2MW, Base wind speed = 10m/s, Maximum power at base wind speed = 1pu, Base rotation speed = 1.2pu.
RSC	R_{igbt} = 1mΩ, K_{pi} = 0.1361, K_{ii} = 2.7221, $i_{d\ ref}$ = 0, f_s = 1350Hz.
GSC	R_{igbt} = 1mΩ, K_{pv} = 8, K_{iv} = 400, K_{pg} = 0.83,K_{ig} = 5, fs = 2250Hz.
Adaptive Fuzzy PID	K_p = 2, K_i = 400, K_d = 0.1

The simulation sets different operating conditions like variable wind speeds and momentary faults on the grid side for comparative analysis and performance validation of the wind farm. Initially, the wind farm is set with different wind speeds that vary with respect to time. The wind speed changes from 10m/s to 13m/s at 10sec and from 13m/s to 8m/s at 20sec in the 30sec simulation time. All the wind farm's voltages, currents, and powers are recorded and plotted with respect to the time given to each condition.

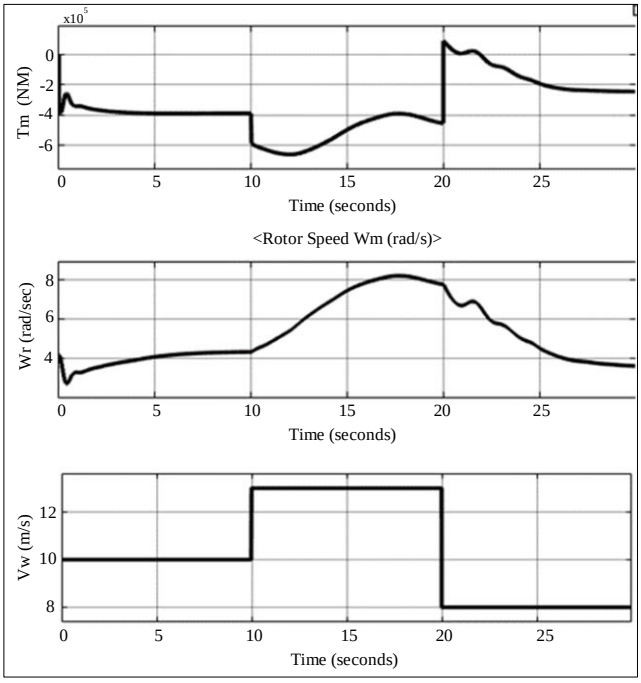

Fig. 6 PMSM characteristics with variable wind speeds

Figure 6 represents the characteristics of PMSM with variable wind speed, as mentioned before, at different instants of time. The Mechanical Torque (Tm) changes according to the wind speed, which impacts the machine's angular speed (wr). As per the change in Tm, the machine's power output is changing. Regarding the change in Tm, the active and reactive power outputs of the PMSM based wind farm are presented in Figure 7.

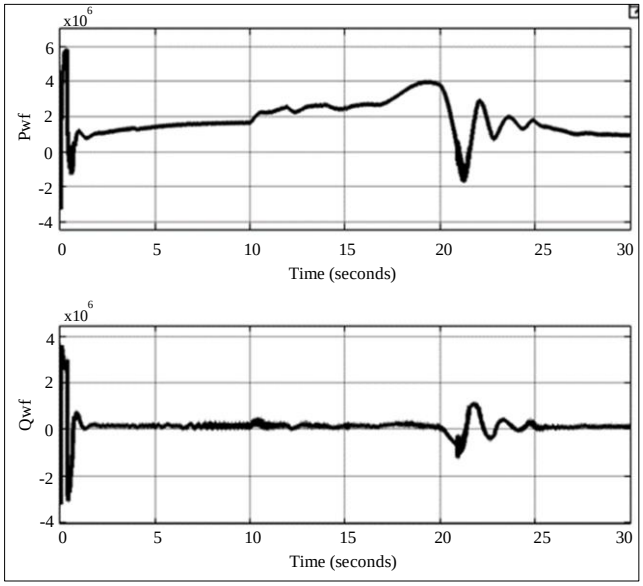

Fig. 7 Active and reactive powers of wind farms as per change in wind speed

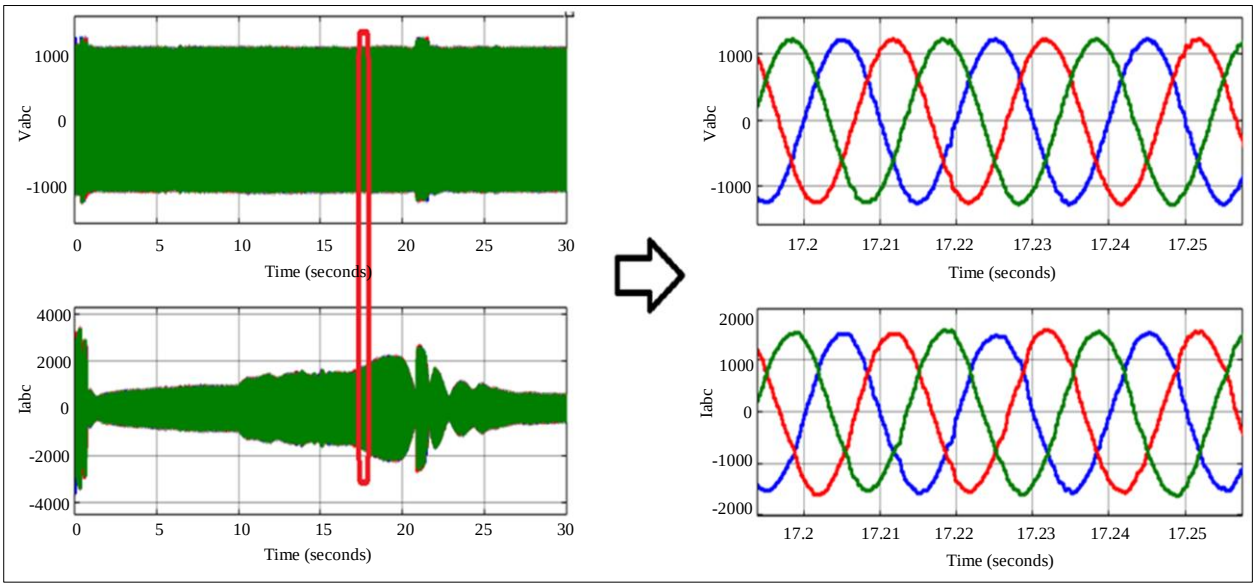

Fig. 8 Three phase voltages and currents of wind farm with change in wind speeds

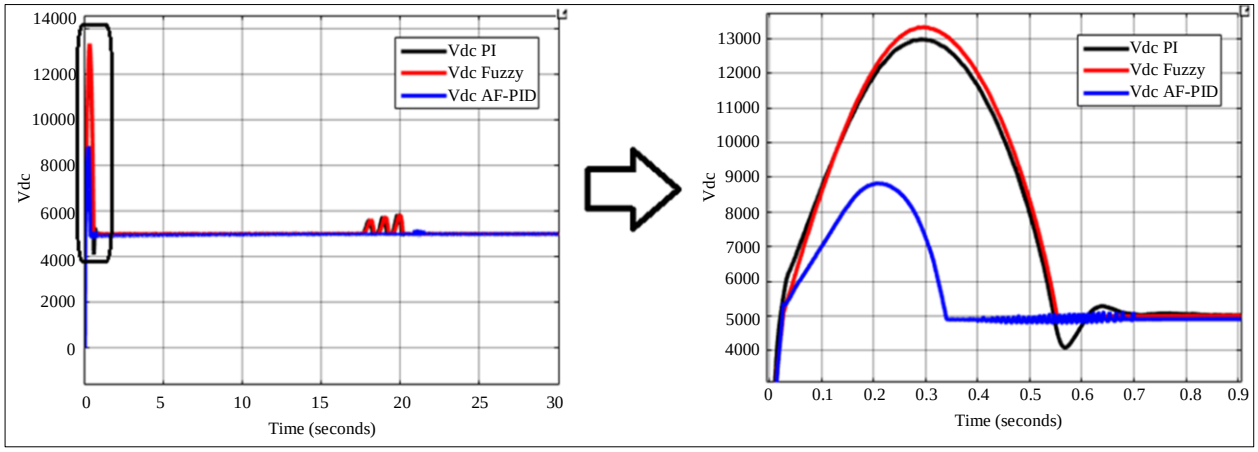

Fig. 9 DC link voltage comparison for variable wind speeds

The active power varies according to the wind speed; however, the reactive power always maintains at zero to avoid reactive power exchange. For the same operating condition, the three phase voltages and currents at the output of the wind generator are presented in Figure 8.

As observed in Figure 8, the voltages are always stable in any operating state, whereas the injected current changes according to the wind speed. The zoomed graph on the right shows near to Sinusoidal waveforms of the voltages and current of the wind generator.

Figure 9 is the DC link voltage comparison measured across the capacitor between the back-to-back connected VSCs. A comparison is made between conventional PI, Fuzzy and Adaptive Fuzzy PID DC voltage regulators. As observed, there is a significant decrease in peak overshoot and settling time when the wind farm is operated with an Adaptive Fuzzy PID regulator. Regarding the same comparison, the characteristics of wind farms are presented in the Figure 10.

It is observed that the characteristics of the wind farm are more stable when operated with an Adaptive Fuzzy PID regulator than those of conventional regulators. A momentary three-phase to ground fault is introduced on the grid side from 15 – 15.1sec to observe the wind farm's performance for any other condition. The same graphs of the system's voltage, currents and powers are taken with a constant wind speed of 10m/s and fault on the grid. Figure 11 shows the characteristics of the PMSM with constant wind speed and fault on the grid. It is observed that due to the robustness of the wind farm, the Tm and wr of the machine are not impacted. However, disturbances occurred in the wind farm's active and reactive power injection, as presented in Figure 12.

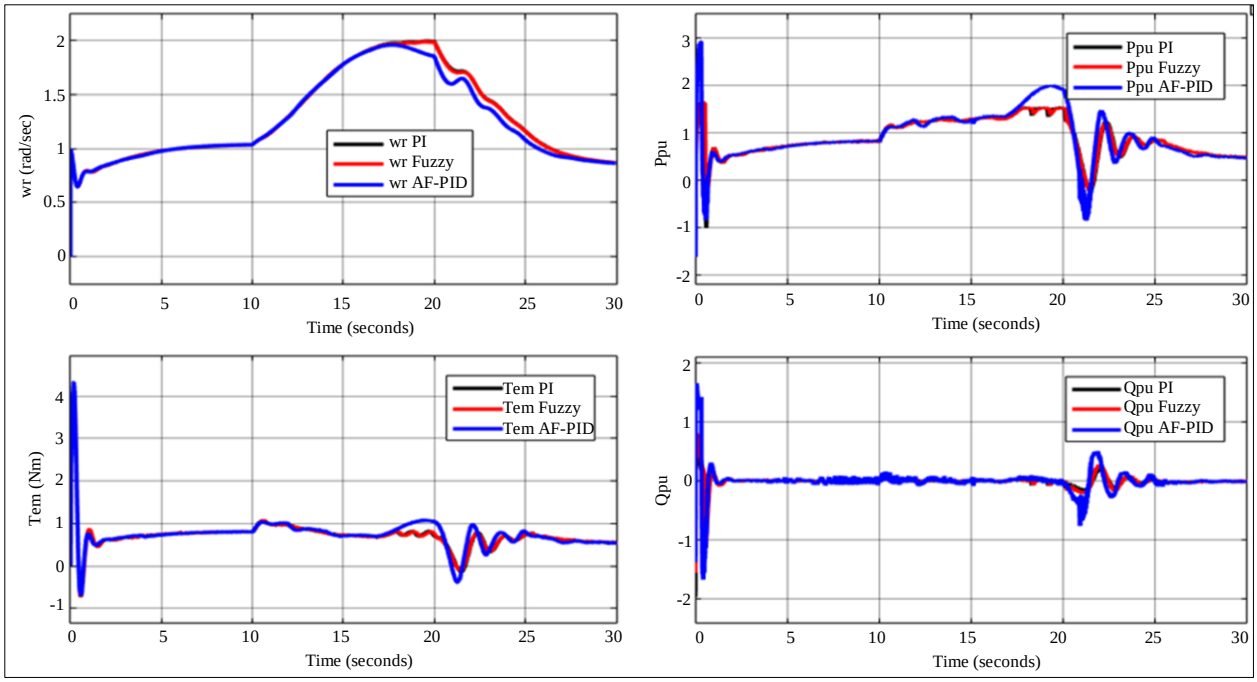

Fig. 10 Wind farm parameters comparison with variable wind speeds

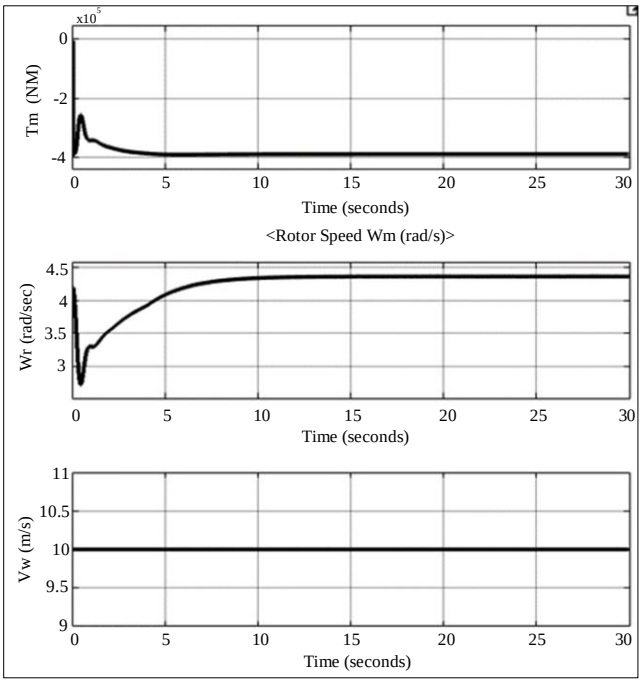

Fig. 11 PMSM characteristics with constant wind speed and momentary fault on grid

The active power drops to a very low value during the fault, which recovers to the rated value just after 0.1 seconds of the fault. This shows the response and performance of the non-linear backstepping controller with an Adaptive Fuzzy PID regulator. For the same condition, the three phase voltages and current of the wind farm are presented in Figure 13.

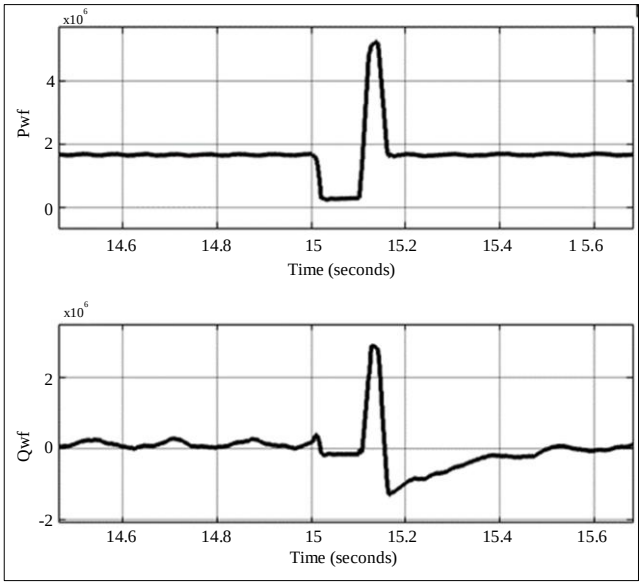

Fig. 12 Active and reactive powers of wind farm with constant wind speed and momentary fault on the grid

As per the given fault at 15sec, the wind farm's voltage completely drops near zero, which shows a drastic rise in current from 15 – 15.1sec. However, after the fault, the voltages and currents get back to their rated values. Figure 14 represents the DC link voltage comparison with the fault introduced on the grid condition.

As per the presented Figure 14, the DC link voltage recovers faster when the GSC controller is updated to an Adaptive Fuzzy PID regulator. This shows the optimal

performance of the controller for the fault conditions created on the grid side. Figure 15 has the comparative graphs of the wind farm parameters for the same fault condition. With different regulators, the Total Harmonic Distortion (THD) of stator currents of the PMSM is calculated using the FFT analysis tool available in the 'powergui' tool presented in Figure 16.

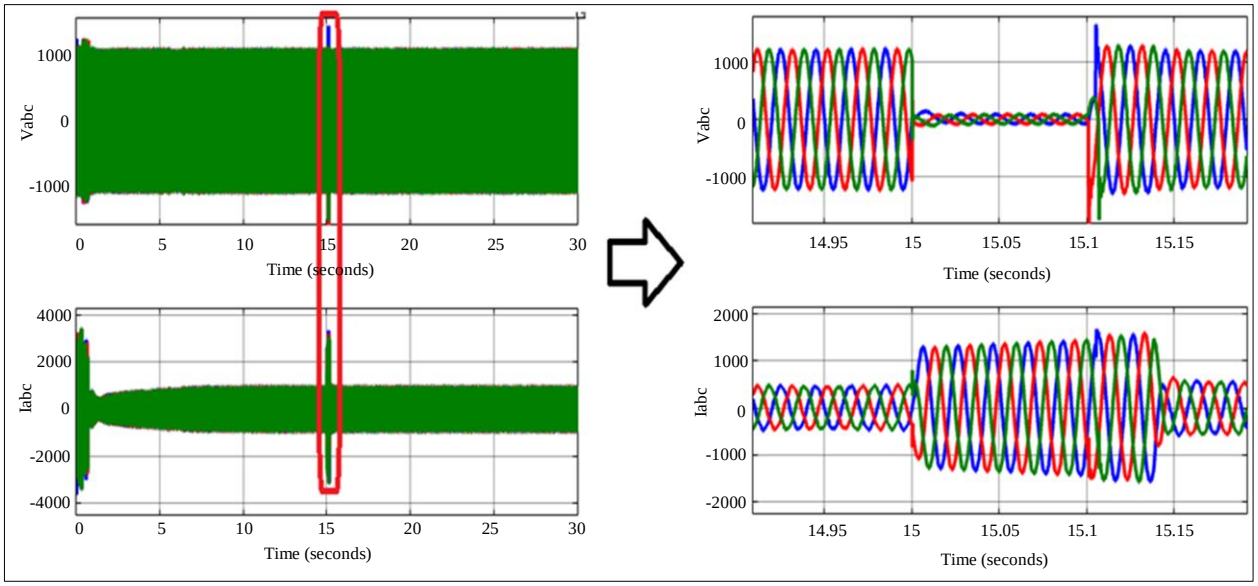

Fig. 13 Three phase voltages and currents of wind farm with constant wind speed and momentary fault on grid

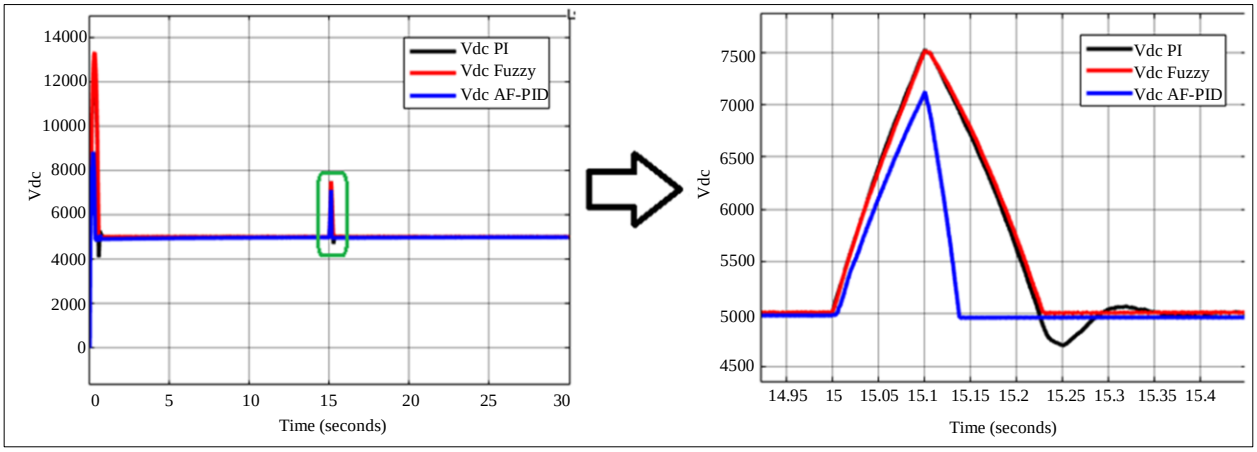

Fig. 14 DC link voltage comparison with constant wind speed and momentary fault on grid

Table 4. Comparison table

Name of the Parameter	PI	Fuzzy	AF-PID
Initial DC Link Voltage Peak	13000V	12500V	8800V
Initial DC Link Voltage Settling Time	0.7sec	0.53sec	0.33sec
Fault DC Link Voltage Peak	7500V	7500V	7000V
Fault DC Link Voltage Settling Time	0.25sec	0.13sec	0.03sec
THD of Stator Current	7.9%	7.94%	4.83%
THD Wind Farm Voltage	4.94%	2.65%	1.58%
THD of Wind Farm Current	5.66%	4.44%	2.58%

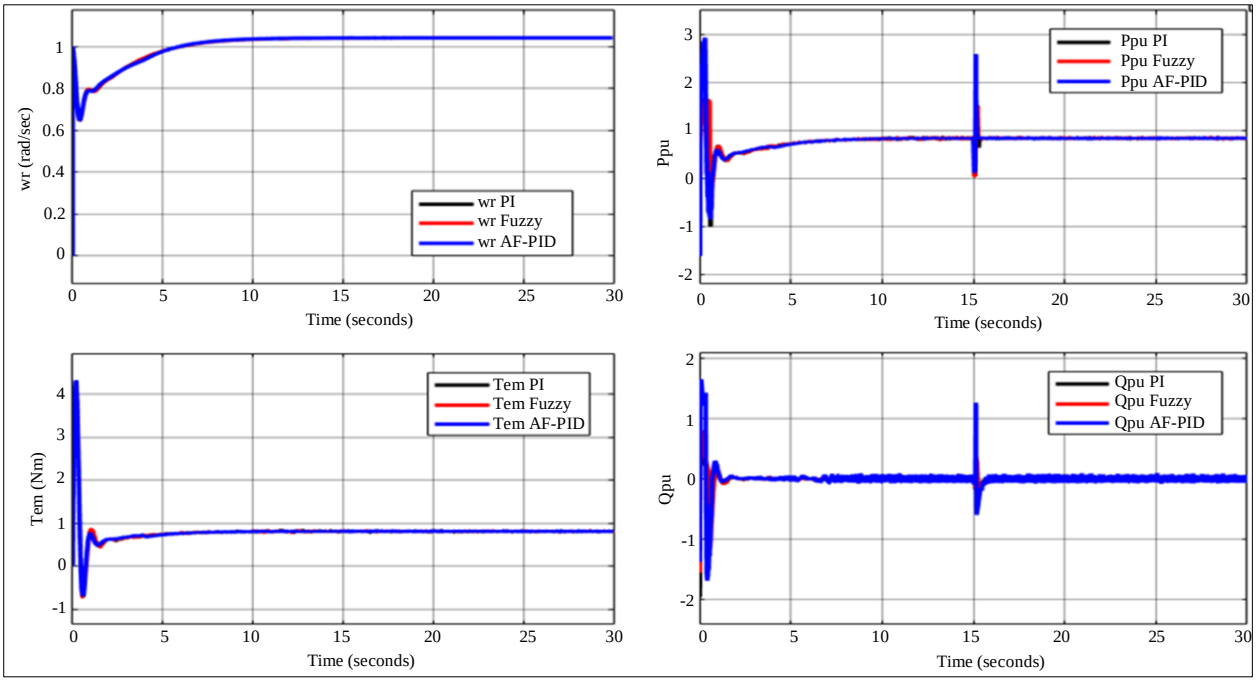

Fig. 15 Wind farm parameters comparison with constant wind speed and momentary fault on grid

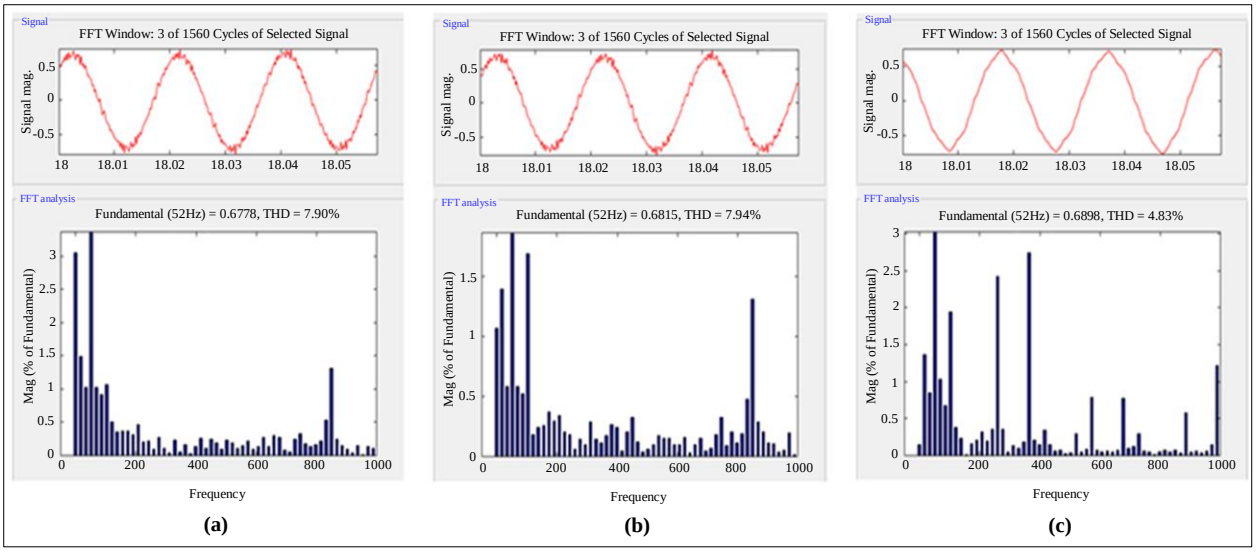

Fig. 16 THDs of the PMSM stator current with the (a) PI regulator, (b) Fuzzy regulator, and (c) Adaptive fuzzy PID regulator.

It can be observed that the harmonics in the stator current of the PMSM, when operated with an Adaptive Fuzzy PID controller, have the lowest harmonic content compared to PI and Fuzzy regulators. A parametric comparison table 4 is presented, validating the performance of the wind farm with different regulators operating in different operating conditions.

5. Conclusion

The PMSM-based wind turbine generator is considered to be the most robust and independent wind farm because of its structural and placement advantages. The power generation during the initial stage shows the response and wind farm. With the non-linear backstepping controllers in the GSC and MSC control structures, the proposed topology is more stable and responds faster to changes in the system and environmental parameters. When the GSC controller of the wind farm is updated with an Adaptive Fuzzy PID regulator, there is a drastic variation in the performance of the topology. Due to the updated voltage regulator, there is a significant drop of 32% in the initial peak overshoot DC link voltage value. Along with this, the initial settling time of the DC link voltage also decreases by 37%, which significantly enhances the system. Even during a fault on the grid, the DC link voltage

recovers faster with an Adaptive Fuzzy PID controller with less voltage overshoot. There is also mitigation of harmonic content in the stator currents, PCC voltages and wind farm injected currents. In any operating condition, the harmonics of the voltages and currents are maintained below 5% as per IEEE 519-2022 low voltage range standard.

References

[1] Subhashish Dey et al., "Renewable Energy Present Status and Future Potentials in India: An Overview," *Innovation and Green Development*, vol. 1, no. 1, 2022. [CrossRef] [Google Scholar] [Publisher Link]

[2] Tze-Zhang Ang et al., "A Comprehensive Study of Renewable Energy Sources: Classifications, Challenges and Suggestions," *Energy Strategy Reviews*, vol. 43, 2022. [CrossRef] [Google Scholar] [Publisher Link]

[3] Phebe Asantewaa Owusu, Samuel Asumadu-Sarkodie, and Shashi Dubey, "A Review of Renewable Energy Sources, Sustainability Issues and Climate Change Mitigation," *Cogent Engineering*, vol. 3, no. 1, 2016. [CrossRef] [Google Scholar] [Publisher Link]

[4] M.Q. Duong et al., "Performance Analysis of Grid-Connected Wind Turbines," *UPB Scientific Bulletin, Series C: Electrical Engineering and Computer Science*, vol. 76, no. 4, pp. 169-180, 2014. [Google Scholar] [Publisher Link]

[5] Mohamed E. Abdallah et al., "Wind Turbine Emulation Using Permanent Magnet Synchronous Motor," *Journal of Electrical Systems and Information Technology*, vol. 5, no. 2, pp. 121-134, 2018. [CrossRef] [Google Scholar] [Publisher Link]

[6] Tim D. Strous, Henk Polinder, and Jan A. Ferreira, "Brushless Doubly-Fed Induction Machines for Wind Turbines: Developments and Research Challenges," *IET Electric Power Applications*, vol. 11, no. 6, pp. 991–1000, 2017. [CrossRef] [Google Scholar] [Publisher Link]

[7] Marcin Lefik et al., "Selecting the Best Permanent Magnet Synchronous Machine Design for Use in a Small Wind Turbine," *Electronics*, vol. 13, no. 10, 2024. [CrossRef] [Google Scholar] [Publisher Link]

[8] Youness Atifi et al., "Nonlinear Control of a Wind Turbine System Connected to the Grid," *IFAC-PapersOnLine*, vol. 58, no. 13, pp. 563-568, 2024. [CrossRef] [Google Scholar] [Publisher Link]

[9] Louar Fateh et al., "Modeling and Control of a Permanent Magnet Synchronous Generator Dedicated to Standalone Wind Energy Conversion System," *Frontiers in Energy*, vol. 10, 155-163, 2016. [CrossRef] [Google Scholar] [Publisher Link]

[10] Zenachew Muluneh Hailemariam, Roberto Leidhold, and Gebremichael Teame Tesfamariam, "Real-Time Speed Control of a PMSM for Wind Turbine Application," *2019 IEEE PES/IAS Power Africa*, Abuja, Nigeria, pp. 396-401, 2019. [CrossRef] [Google Scholar] [Publisher Link]

[11] Hafid Ben Achour, Said Ziani, and Youssef El Hassouani, "A Non-Linear Backstepping Control of Permanent Magnet Synchronous Motor (PMSM)," *International Conference on Connected Object and Artificial Intelligence*, vol. 52, 2023. [CrossRef] [Google Scholar] [Publisher Link]

[12] A. Senhaji et al., "Backstepping Control of a Permanent Magnet Synchronous Motor," *Materials Today: Proceedings*, vol. 72, part 7, pp. 3730-3737, 2023. [CrossRef] [Google Scholar] [Publisher Link]

[13] Jiandong Duan, Shuai Wang, and Li Sun, "Backstepping Sliding Mode Control of a Permanent Magnet Synchronous Motor Based on a Nonlinear Disturbance Observer," *Applied Sciences*, vol. 12, no. 21, 2022. [CrossRef] [Google Scholar] [Publisher Link]

[14] Fayez F.M. El-Sousy, and Khaled A. Abuhasel, "Nonlinear Adaptive Backstepping Control-Based Dynamic Recurrent RBFN Uncertainty Observer for High-Speed Micro Permanent-Magnet Synchronous Motor Drive System," *2018 IEEE Energy Conversion Congress and Exposition (ECCE)*, Portland, OR, USA, pp. 1696-1703, 2018. [CrossRef] [Google Scholar] [Publisher Link]

[15] Tingting Wang et al., "An Adaptive Fuzzy PID Controller for Speed Control of Brushless Direct Current Motor," *SN Applied Sciences*, vol. 4, 2022. [CrossRef] [Google Scholar] [Publisher Link]

[16] Maneesh Kumar et al., "An Adaptive Fuzzy Controller-Based Distributed Voltage Control Strategy for a Remote Microgrid System with Solar Energy and Battery Support," *IEEE Transactions on Industry Applications*, vol. 60, no. 3, pp. 4870-4887, 2024. [CrossRef] [Google Scholar] [Publisher Link]

[17] Yuanhui Yang et al., "A New Type of Adaptive Fuzzy PID Controller," *2010 8th World Congress on Intelligent Control and Automation*, Jinan, China, pp. 5306-5310, 2010. [CrossRef] [Google Scholar] [Publisher Link]

[18] R. Kandiban, and R. Arulmozhiyal, "Speed Control of BLDC Motor Using Adaptive Fuzzy PID Controller," *Procedia Engineering*, vol. 38, pp. 306-313, 2012. [CrossRef] [Google Scholar] [Publisher Link]

[19] Krasimir Ormandzhiev, and Stanimir Yordanov, "Design of Adaptive Fuzzy PID Controller for Electropneumatic System," *25th Scientific Conference on Power Engineering and Power Machines*, vol. 207, 2020. [CrossRef] [Google Scholar] [Publisher Link]